

Proceedings of the
CENTRE FOR MATHEMATICS
AND ITS APPLICATIONS
AUSTRALIAN NATIONAL UNIVERSITY

Volume 38, 2000

NEMACOM
New Methods in Applied and Computational
Mathematics Workshop
(Queensland, July, 1998)

Edited by
Roderick Melnik, Suely Oliveira and David Stewart

Approximate Models of Dynamic Thermoviscoelasticity Describing Shape-Memory-Alloy Phase Transitions

R.V.N. Melnik and A.J. Roberts

*Department of Mathematics and Computing, University of Southern Queensland, Toowoomba,
QLD 4305, Australia.*

1. Introduction

In this paper we consider two models for the approximate description of thermomechanical behaviour of viscoelastic materials. Accounting for thermal fields in such a description is important for all viscoelastic materials ranging from viscous fluids to elastic solids. The viscoelastic behaviour typically combines viscous and elastic properties and the relative proportion of this combination strongly depends on thermal characteristics of the material. Moreover, with changing thermal conditions, it is sometimes difficult to decide whether a particular material is a solid or a fluid. The key points in such decisions belong to the time of observation and to the choice of constitutive relations which couple stresses, deformation gradients, thermal fluxes and temperature.

Our analysis is based on the nonlocal theory of continuum mechanics which considers constitutive variables defined at a point as a function of their values over the whole spatial domain of interest rather than as a function at that point only [2]. This approach of rational mechanics allows us to derive a general model that is suitable for the description of thermomechanical behaviour of materials under a wide range of temperature and loading patterns. In our models we allow for the dependency of stresses not only on the deformation gradient and temperature but also on the rates of their changes. Such considerations put us closer to real situations where the time-dependent coupling between temperature and stresses have to include the velocity of the deformation gradient and the speed of thermal propagation. Another novelty of our paper is the accounting for finite speeds of thermal disturbances. We define the constitutive relationship for thermal fluxes using the Cattaneo-Vernotte equation which includes the classical Fourier law as a special limiting case (in the limit of zero relaxation time for heat fluxes). In particular this approach is critical in modelling short transient states in low temperature regimes.

During recent years a number of papers were devoted to the development of mathematical theory of thermomechanical phase transitions (see [19, 27, 12, 13, 1] and references therein). The majority of those papers dealt with important theoretical issues of models such as well-posedness and the global asymptotic behaviour of solutions. However, only a few papers have been devoted to the description of computational results using those models (see, for example, [20, 15] and references therein). Almost all developed models take into account neither the rate of thermal disturbances nor the relaxation time of thermal fluxes. However, the importance of these issues are well known in dynamic hyperbolic thermoelasticity where mathematical procedures and computational techniques have a longer history compared to that in thermoviscoelasticity [16, 23].

In dealing with the three main physical quantities of continuum mechanics (stresses, deformation gradients and displacements) it is important to take into account their coupling to the thermal field. This allows us to construct efficient mathematical models

for the description of complicated phenomena, such as hysteresis, which are becoming increasingly important in a wide range of applications. In this paper we apply the developed models to the description of shape memory alloy effects in a large bar. It is well-known that for many types of shape memory materials the dependency of stresses on the deformation gradient upon loading and unloading is significantly different. Applying a large load at a low temperature, we may get a residual deformation gradient, which typically vanishes upon heating. The restoring of the original shape is referred to as the shape memory effect. This effect is discussed with two numerical examples.

The rest of the paper is organized as follows.

- Section 2 provides the reader with basic preliminaries and notation.
- The general formulation of the model is given in Section 3. In this section we specify the model for internal energy and derive restrictions on the model imposed by the second law of thermodynamics.
- In Section 4 we incorporate the Cattaneo-Vernotte equation for heat conduction into our model.
- Section 5 deals with the Landau-Devonshire model for the free energy function. The constitutive relation connecting stresses and the deformation gradient is also discussed in this section.
- In Section 6 we consider a one-dimensional model of thermoviscoelasticity and discuss the consequences of non-convexity of free energy function.
- Some numerical results are presented and discussed in Section 7.
- In Section 8 we use centre manifold theory to derive an approximate mathematical model for the description of thermomechanical behaviour of viscoelastic materials.

2. Preliminaries and Notation

Assume that an object of interest (a solid, fluid, gas or plasma) occupies the volume V in a fixed reference spatial configuration Ω at a certain time t_0 . This object in its spatio-temporal configuration will be referred to by the generic name "system". We aim to develop an efficient mathematical description of the dynamic thermomechanical behaviour of the system.

Let $\mathbf{x} = (x_1, x_2, x_3)$ be material (Lagrangian) coordinates of a material point of the system in the configuration Ω at time t_0 . Then the dynamics of the system is determined by the spatial displacements $\mathbf{u} = (u_1, u_2, u_3)$ of such material points as a function of the reference position, \mathbf{x} , and the time of interest, t . The partial derivative of displacement with respect to \mathbf{x} is identified with the symmetric strain tensor

$$\epsilon = \text{sym} \left[\frac{\partial \mathbf{u}(\mathbf{x}, t)}{\partial \mathbf{x}} \right] \quad \text{or} \quad \epsilon_{ij}(\mathbf{x}, t) = \frac{1}{2} \left[\frac{\partial u_i(\mathbf{x}, t)}{\partial x_j} + \frac{\partial u_j(\mathbf{x}, t)}{\partial x_i} \right], \quad i, j = 1, 2, 3, \quad (2.1)$$

and the time derivative of the function \mathbf{u} is identified with the velocity of the system

$$\mathbf{v} = \frac{\partial \mathbf{u}}{\partial t} \quad \text{or} \quad v_i(\mathbf{x}, t) = \frac{\partial u_i(\mathbf{x}, t)}{\partial t}, \quad i = 1, 2, 3. \quad (2.2)$$

In (2.1) we require that $\det(I + \epsilon) > 0$ which precludes a possibility of compression of the matter to zero and guarantees the local invertibility of $\mathbf{x} + \mathbf{u}(\mathbf{x}, t)$ [22]. Since the time derivatives are understood in the Lagrangian sense, \mathbf{x} is kept fixed in (2.2).

3. Nonlocal Models of Thermoviscoelasticity

The equation of motion requires information on forces acting per unit area of the matter and, hence, in a natural way, involves the concept of stresses. The stress is not a mere function of the deformation gradient, as it is often assumed. It also depends on temperature of the matter, its rate of change in time and the rate of change of deformation gradient ϵ . Let $\rho_0(\mathbf{x}, t_0) > 0$ be the density of the matter (the mass per unit volume) in the reference configuration Ω at time t_0 and $\rho(\mathbf{x}, t)$ be the density of the matter at time t where $t - t_0$ is sufficiently small. Then, in the Lagrangian system of coordinates (\mathbf{x}, t) , the equation for balance of mass is written in the form [22]

$$\rho(\mathbf{x}, t) \det(I + \epsilon(\mathbf{x}, t)) = \rho_0(\mathbf{x}, t_0). \quad (3.1)$$

The equation of motion has the following form

$$\rho \frac{\partial^2 \mathbf{u}}{\partial t^2} = \nabla_{\mathbf{x}} \cdot \mathbf{s} + \mathbf{F} \quad \text{with} \quad \mathbf{F} = \rho(\mathbf{f} + \hat{\mathbf{f}}) - \hat{\rho} \mathbf{v}, \quad (3.2)$$

where \mathbf{f} is a given body force per unit mass, $\hat{\rho}$ and $\hat{\mathbf{f}}$ are nonlocal mass and force residuals respectively, and \mathbf{s} is the stress tensor.

In Lagrangian coordinates the equation for energy balance has the form

$$\rho \frac{\partial}{\partial t} \left(e + \frac{\mathbf{v}^2}{2} \right) - \nabla_{\mathbf{x}} \cdot (\mathbf{s} \cdot \mathbf{v}) + \nabla \cdot \mathbf{q} = \rho \left(h + \hat{h} + \mathbf{f} \cdot \mathbf{v} - \frac{\hat{\rho}}{\rho} \left(e + \frac{\mathbf{v}^2}{2} \right) \right), \quad (3.3)$$

where e is the specific internal energy of the system, $\mathbf{v}^2 = \mathbf{v} \cdot \mathbf{v}$, h is the heat source density, \hat{h} is the nonlocal energy residual (see [2] for conditions on localised residuals) and \mathbf{q} is the heat flux. The scalar multiplication of (3.2) by \mathbf{v} gives

$$\rho \frac{\partial \mathbf{v}^2 / 2}{\partial t} - \mathbf{v} \cdot (\nabla \cdot \mathbf{s}) = (\mathbf{F}, \mathbf{v}) \equiv \rho(\mathbf{f} + \hat{\mathbf{f}}) \cdot \mathbf{v} - \hat{\rho} \mathbf{v}^2. \quad (3.4)$$

Taking into account normalisation, from (3.3) and (3.4) we get

$$\rho \frac{\partial e}{\partial t} - \mathbf{s}^T : (\nabla \mathbf{v}) + \nabla \cdot \mathbf{q} = g, \quad (3.5)$$

where $\mathbf{a}^T : \mathbf{b} = \sum_{i,j=1}^3 a_{ij} b_{ij}$ is the standard notation for the rank 2 tensors \mathbf{a} and \mathbf{b} and

$$g = \rho(h + \hat{h}) - \rho \hat{\mathbf{f}} \cdot \mathbf{v} - \hat{\rho} \left(e - \frac{\mathbf{v}^2}{2} \right). \quad (3.6)$$

The right-hand sides of equations (3.2) and (3.5) incorporate into the model nonlocal and dissipative effects of thermomechanical waves. As we shall see in the next section, under appropriate constitutive relations it is also possible to allow for a relaxation time for acceleration of the motion in response to applied gradients such as the deformation gradient and the temperature gradient.

We assume that there exists a one-to-one entropy function of the system state. We denote the density of such a function by η , and then the second law of thermodynamics is

$$\frac{\partial \eta}{\partial t} - \nabla \cdot \mathbf{r} \geq \xi + \hat{\xi} - \frac{\hat{\rho}}{\rho}, \quad (3.7)$$

where ξ is the entropy source density, \mathbf{r} is the entropy flux density and $\hat{\xi}$ is the nonlocal entropy residual.

The system of equations (3.2), (3.5) combined with inequality (3.7) provides the general mathematical model for the description of thermomechanical behaviour of dynamic systems. The macroscopic modelling of such systems starts from the choice of constitutive relationships. We assume the existence of a functional Ψ invariant under a time shift and chose this functional in the form of the Helmholtz free energy

$$\Psi = e - \theta \eta, \quad (3.8)$$

where θ is the temperature of the system ($\theta > 0$, $\inf_{(\mathbf{x}, t)} \theta = 0$). We also assume specific forms for the entropy flux and the entropy source density as

$$\mathbf{r} = \mathbf{q}/\theta, \quad \xi = h/\theta. \quad (3.9)$$

Using (3.8) in (3.5) and taking into account that

$$\nabla \cdot \mathbf{q} = \theta \nabla \cdot (\mathbf{q}/\theta) + (\mathbf{q} \cdot \nabla \theta)/\theta, \quad (3.10)$$

from (3.7) and (3.9) we get the nonlocal formulation of the Clausius-Duhem inequality

$$-\frac{\hat{\rho}}{\rho} \left(\Psi - \frac{\mathbf{v}^2}{2} \right) - \left(\frac{\partial \Psi}{\partial t} + \eta \frac{\partial \theta}{\partial t} \right) + \mathbf{s}^T : \nabla \mathbf{v} - \hat{\mathbf{f}} \cdot \mathbf{v} - \frac{\mathbf{q} \cdot \nabla \theta}{\theta} - (\theta \hat{\xi} - \hat{h}) \geq 0. \quad (3.11)$$

The latter inequality together with requirements on localisation residuals (see [2] for details) impose restrictions on the choice of nonlocal residuals and the functions η , \mathbf{s} and \mathbf{q} . We assume that the entropy density is given in the form

$$\eta = -\frac{\partial \Psi}{\partial \theta}. \quad (3.12)$$

Finally, we have to specify the constitutive relationships that couple stresses, deformation gradients, temperature and heat fluxes

$$\Phi_1(\mathbf{s}, \epsilon) = 0, \quad \Phi_2(\mathbf{q}, \theta) = 0, \quad (3.13)$$

where it is implicitly assumed that these relations may involve spatial and temporal derivatives of the functions. In Section 4 and 5 we specify particular forms for Φ_1 and Φ_2 .

4. The Cattaneo-Vernotte Model for Heat Conduction

The choice of the function Φ_2 in (3.13) is made using the Cattaneo-Vernotte model

$$\mathbf{q} + \tau_0 \frac{\partial \mathbf{q}}{\partial t} = -k(\theta, \epsilon) \nabla \theta, \quad (4.1)$$

where τ_0 is the dimensionless thermal relaxation time and $k(\theta, \epsilon)$ is the thermal conductivity of the material (typically $k = 1 + \tilde{\beta}\theta$ with the given dimensionless coefficient $\tilde{\beta}$). Such a choice is made in order to account for the finite speeds of thermal wave propagation and thermally induced stress wave propagation coupled to the deformation gradient [11, 18]. In order to incorporate equation (4.1) into the general model of thermoviscoelasticity we use a consequence of (3.5)

$$\rho \tau_0 \frac{\partial^2 e}{\partial t^2} - \tau_0 \frac{\partial}{\partial t} [\mathbf{s}^T : (\nabla \mathbf{v})] + \tau_0 \nabla \cdot \left(\frac{\partial \mathbf{q}}{\partial t} \right) = \tau_0 \frac{\partial g}{\partial t}. \quad (4.2)$$

On the other hand, from (4.1) we get

$$\nabla \cdot \mathbf{q} + \tau_0 \nabla \cdot \left(\frac{\partial \mathbf{q}}{\partial t} \right) = -\nabla \cdot (k \nabla \theta). \quad (4.3)$$

Then from (3.5), (4.2), (4.3) we obtain the energy balance equation in the form

$$\rho \frac{\partial e}{\partial t} + \rho \tau_0 \frac{\partial^2 e}{\partial t^2} - \mathbf{s}^T : (\nabla \mathbf{v}) - \tau_0 \frac{\partial}{\partial t} [\mathbf{s}^T : (\nabla \mathbf{v})] - \nabla \cdot (k \nabla \theta) = G, \quad (4.4)$$

where

$$G = g + \tau_0 \frac{\partial g}{\partial t}. \quad (4.5)$$

During recent years, the interest in such a hyperbolic approach in the analysis of materials with memory has increased [6].

5. The Landau-Devonshire Model for the Helmholtz Free Energy and the Stress-Strain Relation

We start from the consideration of the one-dimensional case assuming the following approximation for the free energy of the system

$$\Psi(\theta, \epsilon) = \psi_0(\theta) + \psi_1(\theta)\psi_2(\epsilon) + \psi_3(\epsilon) \quad (5.1)$$

where $\psi_0(\theta)$ models thermal field contributions, $\psi_1(\theta)\psi_2(\epsilon)$ models shape-memory contributions and $\psi_3(\epsilon)$ models mechanical field contributions. These models are chosen in the following forms

$$\begin{cases} \psi_0(\theta) = \alpha_0 - \alpha_1 \theta \ln \theta, & \psi_1(\theta) = \frac{1}{2} \alpha_2 \theta, & \psi_2(\epsilon) = \epsilon^2, \\ \psi_3(\epsilon) = -\frac{1}{2} \alpha_2 \theta_1 \epsilon^2 - \frac{1}{4} \alpha_4 \epsilon^4 + \frac{1}{6} \alpha_6 \epsilon^6, \end{cases} \quad (5.2)$$

where all α_i and θ_1 are positive constants. The model (5.1)–(5.2), known as the Landau-Devonshire model for the Helmholtz free energy, covers a number of important practical cases. However, it belongs to the class of models which is difficult to investigate compared to the Landau-Devonshire-Ginzburg model. In the latter case an additional “smoothing” term in (5.1), known as the Ginzburg term γu_{xxx} , allows us to obtain a bound of the deformation gradient (strain) using a well established technique [5].

Remark 5.1 *A number of important characteristics of phase transformations (such as the size of hysteresis) may depend on the contributions of the interfacial energies. These contributions are often modeled with the Ginzburg correction term. However, the Ginzburg coefficient can only be determined in approximate order [28] and in the general case this coefficient may not be temperature-independent. Another way to account for the contributions of interfacial energies is to take the free energy in the form [4, 17]*

$$\Psi = (1 - z)\tilde{\psi}_1(\epsilon, \theta) + z\tilde{\psi}_2(\epsilon, \theta) + z(1 - z)\tilde{\psi}_3, \quad (5.3)$$

where z is the volume fraction of martensite (i.e. the product phase), $(1 - z)$ is the volume fraction of austenite (i.e. the parent phase), $\tilde{\psi}_1, \tilde{\psi}_2$ are the free energies of austenite and martensite respectively and $\tilde{\psi}_3$ is the contribution from the interaction effect between austenite and martensite. We will not pursue these ideas in this paper.

Remark 5.2 *Some authors include a linear term $\alpha^0\theta$ into $\psi_0(\theta)$. This term has no bearing on the final model and changes only the value of the coefficient of θ in the internal energy representation (see formula (6.2)), and thus is omitted.*

In the general case for the choice of the function Φ_1 in (3.13) we allow the dependency of the stress on the rate of temperature and the deformation gradient

$$s = \rho \left[p(\theta, \epsilon) + \lambda \left(\frac{\partial \theta}{\partial t}, \frac{\partial \epsilon}{\partial t} \right) \right], \quad (5.4)$$

where

$$p(\theta, \epsilon) = \frac{\partial \Psi}{\partial \epsilon}, \quad \lambda \left(\frac{\partial \theta}{\partial t}, \frac{\partial \epsilon}{\partial t} \right) = \tilde{\mu}(\theta) \frac{\partial \epsilon}{\partial t} + \tilde{\nu}(\epsilon) \frac{\partial \theta}{\partial t}. \quad (5.5)$$

It is straightforward to deduce

$$p(\theta, \epsilon) = \alpha_2\theta\epsilon + \frac{\partial \psi_3(\epsilon)}{\partial \epsilon} = [\alpha_2\epsilon(\theta - \theta_1) - \alpha_4\epsilon^3 + \alpha_6\epsilon^5]. \quad (5.6)$$

6. One-Dimensional Hyperbolic Approximation of Shape-Memory-Alloy Dynamics

Using the model (5.1) and (5.2), from (3.12) we get

$$\eta = \alpha_1(1 + \ln \theta) - \frac{1}{2}\alpha_2\epsilon^2. \quad (6.1)$$

This enables us to find the internal energy of the system as a sum of thermal and mechanical fields contributions

$$e = \alpha_0 + \alpha_1\theta - \frac{1}{2}\alpha_2\theta_1\epsilon^2 - \frac{1}{4}\alpha_4\epsilon^4 + \frac{1}{6}\alpha_6\epsilon^6 = \alpha_0 + \alpha_1\theta + \psi_3(\epsilon). \quad (6.2)$$

The substitution of (6.2) into (4.4) leads to the final form of the energy balance equation. In particular, assuming symmetry of the deformation gradient tensor, we get

$$\rho\alpha_1 \left[\frac{\partial\theta}{\partial t} + \tau_0 \frac{\partial^2\theta}{\partial t^2} \right] + A(\epsilon, \theta) - \nabla \cdot (k\nabla\theta) = G, \quad (6.3)$$

where the meaning of A is

$$\begin{aligned} A(\epsilon, \theta) = & -\rho\alpha_2 \left\{ \theta\epsilon \frac{\partial\epsilon}{\partial t} + \tau_0 \frac{\partial}{\partial t} \left[\theta\epsilon \frac{\partial\epsilon}{\partial t} \right] \right\} - \rho\tilde{\mu}(\theta) \left\{ \left(\frac{\partial\epsilon}{\partial t} \right)^2 + \right. \\ & \left. \tau_0 \frac{\partial}{\partial t} \left[\left(\frac{\partial\epsilon}{\partial t} \right)^2 \right] \right\} - \rho \frac{\partial\theta}{\partial t} \left\{ \tilde{\nu}(\epsilon) \frac{\partial\epsilon}{\partial t} + \tau_0 \frac{\partial}{\partial t} \left[\tilde{\nu}(\epsilon) \frac{\partial\epsilon}{\partial t} \right] \right\}. \end{aligned} \quad (6.4)$$

Equation (6.3) is solved together with the equation of motion (3.2) with respect to (u, θ) :

$$\begin{cases} C_v \left[\frac{\partial\theta}{\partial t} + \tau_0 \frac{\partial^2\theta}{\partial t^2} \right] - k_1 \left[\theta \frac{\partial u}{\partial x} \frac{\partial^2 u}{\partial t \partial x} + \tau_0 \frac{\partial}{\partial t} \left(\theta \frac{\partial u}{\partial x} \frac{\partial^2 u}{\partial t \partial x} \right) \right] - \mu \left[\left(\frac{\partial^2 u}{\partial t \partial x} \right)^2 + \right. \\ \left. \tau_0 \frac{\partial}{\partial t} \left(\frac{\partial^2 u}{\partial t \partial x} \right)^2 \right] - \nu \left[\frac{\partial\theta}{\partial t} \frac{\partial^2 u}{\partial t \partial x} + \tau_0 \frac{\partial}{\partial t} \left(\frac{\partial\theta}{\partial t} \frac{\partial^2 u}{\partial t \partial x} \right) \right] - \frac{\partial}{\partial x} \left(k \frac{\partial\theta}{\partial x} \right) = G, \\ \rho \frac{\partial^2 u}{\partial t^2} - \frac{\partial}{\partial x} \left[k_1 \frac{\partial u}{\partial x} (\theta - \theta_1) - k_2 \left(\frac{\partial u}{\partial x} \right)^3 + k_3 \left(\frac{\partial u}{\partial x} \right)^5 \right] - \mu \frac{\partial^3 u}{\partial x^2 \partial t} - \nu \frac{\partial^2 \theta}{\partial x \partial t} = F, \end{cases} \quad (6.5)$$

where $C_v = \rho\alpha_1$, $k_1 = \rho\alpha_2$, $k_2 = \rho\alpha_4$, $k_3 = \rho\alpha_6$, $\mu = \rho\tilde{\mu}$, $\nu = \rho\tilde{\nu}$.

The initial conditions for the model (6.5) are chosen in the form

$$u(x, 0) = u^0(x), \quad \frac{\partial u}{\partial t}(x, 0) = u^1(x); \quad \theta(x, 0) = \theta^0(x), \quad \frac{\partial\theta}{\partial t}(x, 0) = \theta^1(x), \quad (6.6)$$

for given functions u^0 , u^1 , θ^0 , θ^1 . There are several distinct choices for boundary conditions to be used in our computational experiments. Mechanical boundary conditions are taken in one of the following forms (L is the length of the structure):

- "stress-free" boundary conditions: $s(0, t) = s(L, t) = 0$;
- "pinned end" boundary conditions: $u(0, t) = u(L, t) = 0$;
- or mixed mechanical boundary condition: $s(0, t) = 0$, $u(L, t) = 0$.

When displacements are given on boundaries, *a priori* bounds on strains are generally unknown which complicates the mathematical analysis of the problem. Computational results presented in Section 7 deal with this case. Thermal boundary conditions are chosen in one of the following form

- “thermal insulation” boundary conditions: $q(0, t) = q(L, t) = 0$, which reduce to $\frac{\partial \theta}{\partial x}(0, t) = \frac{\partial \theta}{\partial x}(L, t) = 0$ for the Fourier law (see (8.2));
- “controlled flux” boundary conditions: $\frac{\partial \theta}{\partial x}(0, t) = 0$, $-k \frac{\partial \theta}{\partial x}(L, t) = \beta[\theta - \theta^0(t)]$;
- or fixed temperature (“uncontrolled energy flow”) boundary conditions: $\theta(0, t) = \theta(L, t) = 0$.

In the last case additional assumptions are needed. By using the Leray-Schauder principle we have analysed the Cauchy problem for nonlinear hyperbolic model of thermoviscoelasticity (6.5). Our procedure makes use of the Lumer-Phillips theorem and the technique developed in [5]. We shall address details of this technique elsewhere.

Our final remark in this section goes to the choice of the function Ψ in the form (5.1) and (5.2) that brings major difficulties in the investigation of the model (6.5). Strictly speaking, the free energy function strongly depends upon the statistics of the phenomenon and has to be derived from a statistical model. Since van der Waals work on statistical mechanics it is a common practice to choose this function as a non-convex function of ϵ [14]. When dealing with shape memory alloys, minima of this function are known to correspond different phases of the material. For example, in the case of three minima, we expect one austenitic and two martensitic phase (see, for example, [8, 19, 28, 12]). Temperature plays a crucial role in the phase transition. Depending on the value of temperature, the material may alternate between a single thermodynamically unstable nonmonotone branch and multiple unstable branches. The character of this instability depends not only on the deformation gradient and temperature, but also on the rates of their changes.

7. Computational Experiments

In this section we present some numerical results on the thermal and mechanical control of a rod ($L = 1\text{cm}$) with a shape-memory-alloy core. The parameters of the Cu-based core are taken as follows

$$k = 1.9 \times 10^{-2} \text{cmg}/(\text{ms}^3\text{K}), \quad \rho = 11.1 \text{g}/\text{cm}^3, \quad C_v = 29 \text{g}/(\text{ms}^2\text{cmK}), \quad \theta_1 = 208\text{K},$$

$$k_1 = 480 \text{g}/(\text{ms}^2\text{cmK}), \quad k_2 = 6 \times 10^6 \text{g}/(\text{ms}^2\text{cmK}), \quad k_3 = 4.5 \times 10^8 \text{g}/(\text{ms}^2\text{cmK}).$$

We use model (6.5) with $\tau_0 = 0 = \mu = \nu = 0$, initial conditions (6.6) and “pinned end & controlled flux” boundary conditions. This model was straightforwardly reduced to a differential-algebraic system in $\pi = (u, v, \theta)^T$ and stress s using second-order accurate spatial differences on staggered grids:

$$D \frac{\partial \pi}{\partial t} = \mathbf{f}, \quad s = k_1(\theta - \theta_1) \frac{\partial u}{\partial x} - k_2 \left(\frac{\partial u}{\partial x} \right)^3 + k_3 \left(\frac{\partial u}{\partial x} \right)^5, \quad (7.1)$$

where D is the diagonal matrix with $\text{diag}(D) = (1, \rho, C_v)$, $\mathbf{f} = (f_1, f_2, f_3)^T$ and

$$f_1 = v, \quad f_2 = \frac{\partial s}{\partial x} + F, \quad f_3 = k \frac{\partial^2 \theta}{\partial x^2} + k_1 \theta \frac{\partial u}{\partial x} \frac{\partial v}{\partial x} + G. \quad (7.2)$$

The developed code is robust and much simpler compared to computational procedures previously reported in the literature for shape-memory alloys [20, 15, 13].

Experiment 1 (thermal control of phase transformations). In this experiment we set uniform forcing $F = 500\text{g}/(\text{ms}^2\text{cm}^2)$ and vary heating conditions given by $G = 375\pi \sin^3(t\pi/6)\text{g}/(\text{ms}^3\text{cm})$. We assume that the initial displacements are given in the form

$$u^0(x) = \begin{cases} -0.11809x, & 0 \leq x \leq 1/6, \\ 0.11809(x - 1/3), & 1/6 \leq x \leq 1/2, \\ 0.11809(2/3 - x), & 1/2 \leq x \leq 5/6, \\ 0.11809(x - 1), & 5/6 \leq x \leq 1 \end{cases} \quad (7.3)$$

and take the initial temperature as $\theta^0 = 200\text{K}$. Figure 1 (obtained with time step $7 \times 10^{-4}\text{ms}$ and space step $1/24\text{cm}$) demonstrates the transformation of $2M^+ + 2M^-$ martensites into an austenite (visible in the region of zero strain and displacements with superposed elastic vibrations as seen most clearly in the velocity field) after sufficient temperature has reached. Then upon cooling we observe a first order (martensitic) transition from the high temperature phase (austenite) to the low temperature phase (martensite). Upon the return to the low temperature regime the stable attractor with this applied

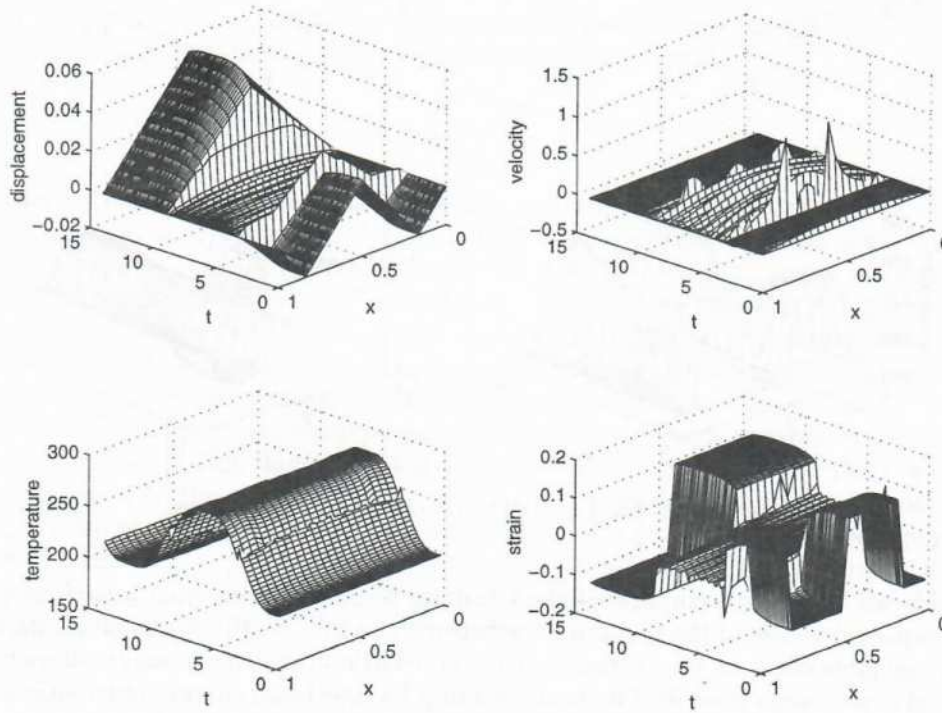


FIGURE 1. Thermally induced phase transformations.

thermomechanical forcing is not the original configuration but only two distinct martensite phases. The transformation $[2M^+ + 2M^-] \rightarrow A$ is accompanied by a decrease in temperature whereas the transformation $A \rightarrow [M^+ + M^-]$ is accompanied by an increase in temperature.

Experiment 2 (mechanical control of phase transformations). In this experiment we set $G = 0$, but vary the mechanical loading according to $F = 7000 \sin^3(\pi t/2)$ g/(cm²ms²). Starting from the austenite configuration ($u^0 = 0$) at intermediate temperature $\theta^0 = 255\text{K}$ we observe (see Figure 2 where the time step was $8 \times 10^{-4}\text{ms}$ and the space step was 1/16cm) the transformation $A \rightarrow [M^+ + M^-] \rightarrow A \rightarrow [M^- + M^+] \rightarrow A$. In this experiment we observe the almost immediate transformations of austenite phases into two martensites upon the increase/decrease in loading. Note the relatively large heating/cooling associated with the transition into/out of martensite phase. A similar behaviour under different thermomechanical conditions was also observed in [20, 15]. In

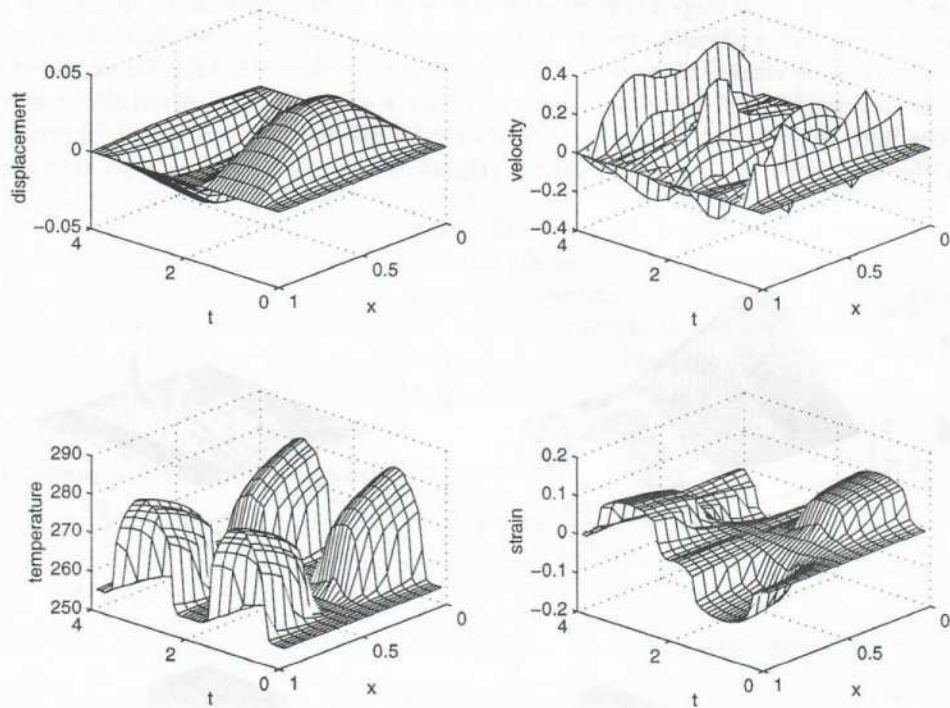


FIGURE 2. Mechanically induced phase transitions.

our code we have also incorporated the Ginsburg term by adding γu_{xxx} to f_2 in (7.2). With reported values of the Ginsburg coefficient ($\gamma \sim 10^{-10} - 10^{-12}$) the Ginsburg term has a negligible effect on the thermomechanical behaviour of shape-memory alloys in the group of experiments described here. Accounting for interfacial energy contributions and the influence of mechanical and thermal dissipations on the dynamics of memory material require further investigation.

8. Construction of Approximate Models for Dynamic Thermoviscoelasticity Using Centre Manifold Theory

The model described in Section 6 will provide a good approximation of thermomechanical behaviour of a large shape memory alloy bar (see applications in [3]) only in the case

the bar can be modelled by a thin rod with a shape memory alloy core. As an alternative to that model, in this section we construct a new model which is derived directly from the 3D model for shape memory alloy evolution (see (3.2), (6.3)) using centre manifold techniques (see, for example, [24]).

We assume that the shear stress in equation (3.2) is determined by its three components, the quasi-conservative component, \mathbf{s}^q , the stress component due to mechanical dissipation, \mathbf{s}^m , and the stress component due to thermal dissipations, \mathbf{s}^t , (the latter is assumed to be negligible at this stage)

$$\mathbf{s} = \mathbf{s}^q + \mathbf{s}^m + \mathbf{s}^t, \quad \text{with} \quad \mathbf{s}^q = \rho \frac{\partial \Psi}{\partial \boldsymbol{\epsilon}}, \quad \mathbf{s}^m = \rho \mu \frac{\partial \boldsymbol{\epsilon}}{\partial t}, \quad \mathbf{s}^t = \mathbf{0}. \quad (8.1)$$

In the general case the heat flux is determined as the solution of equation (4.1). An approximation to this solution is provided by the following generalised form (see [19] and references therein)

$$\mathbf{q} = -k \nabla \theta - \alpha \frac{\partial k \nabla \theta}{\partial t}, \quad \alpha \geq 0, \quad (8.2)$$

which we will use with $\alpha = 0$ when (8.2) turns into the classical Fourier law.

The internal energy function e is defined from (3.8) by

$$e = \Psi - \theta \frac{\partial \Psi}{\partial \theta}. \quad (8.3)$$

In order to complete the formulation of the problem we specify a model for the free energy function Ψ . However, in the general 3D case one cannot use the shear strain as the order parameter as we usually do for the 1D case. One of the first approaches to deal with the 3D challenge was the Frémond model. This model uses different expressions for free energy functions for different phases (see, for example, [10]). All these expressions are essentially of the Landau-Ginsburg-type and contain the term $\gamma/2 \nabla \text{tr}(\boldsymbol{\epsilon})$ with $\gamma > 0$ introduced in order to smooth possibly very sharp spatial phase separation. In this paper we use a different approach proposed in [9]. This approach generalises the classical Landau-Devonshire-Falk theory for shape memory alloys to the 3D case. The free energy function, based on the expansion up to sixth order in a single shear strain component [8], was extended to the three-dimensional case using the group theoretical approach proposed in [21]. In contrast to some other models (see, for example, [10]) strain-gradient terms are not involved in his expansion. We make use of this expansion and apply the following general representation of the free energy function

$$\Psi(\boldsymbol{\epsilon}, \theta) = \psi^0(\theta) + \sum_{n=1}^{\infty} \psi^n(\boldsymbol{\epsilon}, \theta), \quad (8.4)$$

where independent material parameters of the n -th order for $n = 1, 2, \dots$ are determined through strain invariants, \mathcal{I}_j^n , as follows

$$\psi^n = \sum_{j=1}^{j^n} \psi_j^n \mathcal{I}_j^n \quad \text{and} \quad \psi^0(\theta) = \psi_0(\theta). \quad (8.5)$$

The upper limit of the sum in (8.5), j^n , is the number of all invariant directions associated with a representation of the 48th order cubic symmetry group of the parent phase (see details in [9]). In order to adequately describe thermomechanical behaviour of shape-memory alloys we need to account for 6 terms in the sum of the expansion (8.4). In this case we have to determine 32 material parameters that make the application of formulae (8.4)–(8.5) fairly complicated. Using physically justified assumptions it is possible to reduce the number of required parameters. To achieve this, we make the same assumptions as in [9]. They conclude that odd degree invariants can be neglected in the expansion. Taking invariants up to the sixth order results in a representation with only 10 material constants which may depend on temperature

$$\Psi = \psi^0(\theta) + \sum_{j=1}^3 \psi_j^2 \mathcal{I}_j^2 + \sum_{j=1}^5 \psi_j^4 \mathcal{I}_j^4 + \sum_{j=1}^2 \psi_j^6 \mathcal{I}_j^6 \quad (8.6)$$

(we do not neglect the contribution of $\psi^0(\theta)$ as was done in [9]). The strain invariants \mathcal{I}_i^n of second, forth and sixth orders of the 48th order cubic symmetry group of the parent phase are

$$\begin{aligned} \mathcal{I}_1^2 &= \frac{1}{9}(\text{tr}(\epsilon_{ij}))^2, \quad \mathcal{I}_2^2 = \frac{1}{12}(2\epsilon_{33} - \epsilon_{11} - \epsilon_{22})^2 + \frac{1}{4}(\epsilon_{11} - \epsilon_{22})^2, \\ \mathcal{I}_3^2 &= \epsilon_{23}^2 + \epsilon_{13}^2 + \epsilon_{12}^2, \quad \mathcal{I}_1^4 = (\mathcal{I}_2^2)^2, \quad \mathcal{I}_2^4 = \epsilon_{23}^4 + \epsilon_{13}^4 + \epsilon_{12}^4, \quad \mathcal{I}_1^6 = (\mathcal{I}_2^2)^3 \\ \mathcal{I}_3^4 &= (\mathcal{I}_3^2)^2, \quad \mathcal{I}_4^4 = \mathcal{I}_2^2 \mathcal{I}_3^2, \quad \mathcal{I}_5^4 = \epsilon_{23}^2 \left[\frac{1}{6}(2\epsilon_{33} - \epsilon_{11} - \epsilon_{22}) - \frac{1}{2}(\epsilon_{11} - \epsilon_{22}) \right]^2 + \\ &\quad \epsilon_{13}^2 \left[\frac{1}{6}(2\epsilon_{33} - \epsilon_{11} - \epsilon_{22}) + \frac{1}{2}(\epsilon_{11} - \epsilon_{22}) \right]^2 + \frac{1}{9}\epsilon_{12}^2(2\epsilon_{33} - \epsilon_{11} - \epsilon_{22})^2, \\ \mathcal{I}_2^6 &= \frac{1}{36}(2\epsilon_{33} - \epsilon_{11} - \epsilon_{22})^2 \left(\frac{1}{36}(2\epsilon_{33} - \epsilon_{11} - \epsilon_{22})^2 - \frac{1}{4}(\epsilon_{11} - \epsilon_{22})^2 \right)^2. \end{aligned} \quad (8.7)$$

The ten material constants ψ_j^n in (8.6) differ from alloy to alloy and we use coefficients derived for Cu-based alloys [9] (units used here are consistent with those used in Section 7 for our numerical results on the dynamics of shape-memory alloys):

$$\begin{aligned} \psi_1^2 &= 5.92 \times 10^6 \text{ g}/(\text{ms}^2\text{cm}), \quad \psi_2^2 = (1.41 \times 10^5 + 46(\theta - 300)) \text{ g}/(\text{ms}^2\text{cm}), \\ \psi_3^2 &= (1.48 \times 10^6 - 940(\theta - 300)) \text{ g}/(\text{ms}^2\text{cm}), \quad \psi^0 = -\alpha_1 \theta \ln[(\theta - \theta_0)/\theta_0] \text{ g}/(\text{ms}^2\text{cm}), \\ \psi_1^4 &= (-1.182 \times 10^8 + 3.55 \times 10^5(\theta - 300)) \text{ g}/(\text{ms}^2\text{cm}), \\ \psi_2^4 &= 3.13 \times 10^9 \text{ g}/(\text{ms}^2\text{cm}), \quad \psi_3^4 = 1.64 \times 10^9 \text{ g}/(\text{ms}^2\text{cm}), \\ \psi_4^4 &= -5.53 \times 10^8 \text{ g}/(\text{ms}^2\text{cm}), \quad \psi_5^4 = -4.27 \times 10^8 \text{ g}/(\text{ms}^2\text{cm}), \\ \psi_1^6 &= 3.35 \times 10^{10} \text{ g}/(\text{ms}^2\text{cm}), \quad \psi_2^6 = 3.71 \times 10^{11} \text{ g}/(\text{ms}^2\text{cm}). \end{aligned} \quad (8.8)$$

Other material parameters are taken to be the same as those given in Section 7. We are interested in the construction of an adequate model for the description of thermomechanical behaviour of thin slabs in shape memory alloy materials. Starting from the

3D Falk-Konopka model and using centre manifold techniques (see, for example, [24]) we derive systematically an accurate low-dimensional model for the dynamics of the slab. The shape memory alloy is assumed to be of very large extent in the $x = x_1$ direction compared to its thickness of $2b$ in the $y = x_2$ direction ($-b < y < b$). For the sake of convenience we use a new temperature variable $\theta' = \theta - \theta_0$ where here $\theta_0 = 300$. For simplicity of the analysis we assume zero dissipation, $\alpha = \mu = 0$, and that there is no motion nor dependence in the x_3 direction.

A model for the dynamics of modes which vary slowly along the slab is derived for the unforced dynamics, $\mathbf{F} = \mathbf{0}$, $G = 0$, and when "zero-stress & thermal-insulation" boundary conditions are specified on $y = \pm b$. The derivation of boundary conditions in the "long" direction x requires a quite delicate analysis [25] and these issues will not be address here. We only note that "pinned & insulating ends" boundary conditions may be used as a leading approximation. Modelling the long-wavelength, small-wavenumber modes along the slab, we neglect all longitudinal variations and look for eigenvalues of the cross-slab modes. It can be shown that generally there is a zero eigenvalue of multiplicity five and all the rest are pure imaginary (as dissipation has been omitted). Thus there exists a sub-centre manifold based upon these five modes (see [26] for an existence theorem), called a slow manifold as these five modes evolve slowly. Note that being on a sub-centre manifold the models we construct only have a weak assurance of asymptotic completeness, see the discussion in [7]. The zero eigenvalue of multiplicity five corresponds to longitudinal waves, large-scale bending, and one heat mode. The leading order structure of the critical eigenmodes are constant across the slab. Thus letting an overbar denote the y average, the amplitudes of the critical modes are chosen in the form

$$U_i(x, t) = \bar{u}_i, \quad V_i(x, t) = \bar{v}_i, \quad \Theta'(x, t) = \bar{\theta}'. \quad (8.9)$$

The low-dimensional model below is written in terms of these parameters.

The construction of the low-dimensional model is based upon the ansatz that there exists a low-dimensional invariant manifold upon which the amplitudes evolve slowly:

$$u_i = \mathcal{U}_i(\mathbf{U}, \mathbf{V}, \Theta'), \quad v_i = \mathcal{V}_i(\mathbf{U}, \mathbf{V}, \Theta'), \quad \theta = \mathcal{T}(\mathbf{U}, \mathbf{V}, \Theta'), \quad (8.10)$$

$$\text{where} \quad \frac{\partial U_i}{\partial t} = V_i, \quad \frac{\partial V_i}{\partial t} = g_i(\mathbf{U}, \mathbf{V}, \Theta'), \quad \frac{\partial \Theta'}{\partial t} = g_\theta(\mathbf{U}, \mathbf{V}, \Theta'). \quad (8.11)$$

This ansatz is substituted into the differential-algebraic equations of 3D thermo-viscoelasticity (3.2), (3.5) and is solved to some order in the small parameters ∂_x , $E = \|\mathbf{U}_x\| + \|\mathbf{V}_x\|$ and $\vartheta = \|\Theta'\|$ with the computer algebra package Reduce. Thus, here we treat the strains as small, as measured by E , while permitting asymptotically large displacements and velocities. The displacement and temperature fields of the slow manifold, in terms of the amplitudes and the scaled transverse coordinate $Y = y/b$, are approximately

$$u_1 \approx U_1 - YbU_{2x} + 0.15(3Y^2 - 1)b^2U_{1xx}, \quad (8.12)$$

$$u_2 \approx U_2 - (0.9 - 3.05e-5\Theta')YbU_{1x} + 0.15(3Y^2 - 1)b^2U_{2xx} \\ - 141YbU_{1x}^3 + 1.00e-4(3Y - Y^3)b^3V_{1x}^2U_{1x}, \quad (8.13)$$

$$\theta \approx 300 + \Theta' - 2.43e6(3Y - Y^3)b^3(V_{1x}U_{2xx} + U_{1x}V_{2xx}) \\ - 25.1(7 - 30Y^2 + 15Y^4)V_{1x}^3U_{1x}. \quad (8.14)$$

These expressions have errors $\mathcal{O}(E^5 + \partial_x^{5/2} + \vartheta^{5/2})$ where the notation $\mathcal{O}(E^p + \partial_x^q + \vartheta^r)$ is used to denote terms involving $\partial_x^b E^a \vartheta^c$ such that $a/p + b/q + c/r \geq 1$. The mechanical and thermal field approximations represented by (8.12)–(8.14) have cross-slab structure. In particular, the sideways deformation u_2 (which is a nonlinear function of the longitudinal strains) of the shape memory alloy feed back at higher order to contribute to and complicate the longitudinal and thermal dynamics.

The model for the longitudinal dynamics on this slow manifold is

$$\begin{aligned} \rho \frac{\partial V_1}{\partial t} = & 2.97e6 U_{1xx} + 8.03e5 b^2 U_{1xxxx} \\ & + \partial_x \left[(922 \Theta' - 0.0145 \Theta'^2) U_{1x} - (4.28e9 - 1.31e7 \Theta') U_{1x}^3 + 7.12e11 U_{1x}^5 \right. \\ & + (2820 - 8.80 \Theta') b^2 V_{1x}^2 U_{1x} + 1.24 b^4 V_{1x}^4 U_{1x} - 5.42e4 b^2 V_{1x}^2 U_{1x}^3 \left. \right] \\ & + \mathcal{O}(E^8 + \partial_x^4 + \vartheta^4). \end{aligned} \quad (8.15)$$

The first line in the right-hand side of (8.15) describes linear dispersive elastic waves along the slab, whereas the second line gives the temperature dependent quintic stress-strain relation of the shape memory alloy. Since $V_{1x} = U_{1xt}$, the remaining lines show effects upon this stress-strain relation due to rates of change of the strain.

Note that to this order of truncation there is no coupling to the bending modes of the slab which to the same error is simply the beam equation

$$\rho \frac{\partial V_2}{\partial t} = -9.91e5 b^2 U_{2xxx} + \mathcal{O}(E^8 + \partial_x^4 + \vartheta^4). \quad (8.16)$$

There exists nonlinear coupling between the modes at higher order.

The corresponding energy equation for the temperature is

$$\begin{aligned} C_v \frac{\partial \Theta'}{\partial t} = & \kappa \Theta'_{xx} + (2.77e5 + 914 \Theta' - 9.25 \Theta'^2) U_{1x} V_{1x} \\ & + (3.94e9 + 1.26e7 \Theta') V_{1x} U_{1x}^3 - (57.3 + 0.0117 \Theta') b^2 V_{1x}^3 U_{1x} \\ & + 1.68e12 V_{1x} U_{1x}^5 - 1.58e6 b^2 V_{1x}^3 U_{1x}^3 - 0.0203 b^4 V_{1x}^5 U_{1x} \\ & + 1.63e4 b^2 U_{1xx} V_{1xx} + 9.22e4 b^2 U_{2xx} V_{2xx} + \partial_x^2 \left[-8151 b^2 U_{1x} V_{1x} \right] \\ & + \mathcal{O}(E^8 + \partial_x^4 + \vartheta^4). \end{aligned} \quad (8.17)$$

The first line in (8.17) describes the diffusion of heat generated or absorbed by mechanical strains, $\Theta U_{1x} V_{1x}$. However, in the thin slab the internal pattern of strains causes a much more complicated distribution of heating and cooling as summarised by the remaining lines. It is expected that virtually all of these should be retained in order to be consistent with the quintic stress-strain of the longitudinal wave equation. Computational experiments with the model derived in this section will be presented elsewhere.

9. Acknowledgements

The authors were supported by ARC Small Grant 179406. Special thanks go to Kerry Thomas who contributed the results of computational experiments.

References

- [1] Anderssen, R.S., Götz, I. G. and K.-H. Hoffmann, The Global Behaviour of Elasto-Plastic and Visco-Elastic Materials with Hysteresis-Type State Equation, *SIAM J. Appl. Math.*, to appear.
- [2] Balta, F. and Suhubi, E. S., Theory of Nonlocal Generalised Thermoelasticity, *Int. J. Engng. Sci.*, **15**, 1977, 579–588.
- [3] Besselnik, P.A., Recent Development on Shape Memory Applications, *J. Phys. IV France, Colloque C5*, **7**, 1997, 581–590.
- [4] Bornert, M. & Muller, I., Temperature Dependence of Hysteresis in Pseudoelasticity, in *Free Boundary Value Problems*, Eds. K.-H. Hoffmann & J. Sprekels, Birkhauser Verlag, Basel, 1990, 27–35.
- [5] Chen, Z. and K.-H. Hoffmann, On a One-Dimensional Nonlinear Thermoviscoelastic Model for Structural Phase Transitions in Shape Memory Alloys, *Journal of Differential Equations*, **112**, 1994, 325–350.
- [6] Colli, P. and Grasselli, M., Justification of a Hyperbolic Approach to Phase Changes in Materials with Memory, *Asymptotic Analysis*, **10**, 1995, 303–334.
- [7] Cox, S.M. and Roberts, A.J., Initial conditions for models of dynamical systems, *Physica D*, **85**, 1995, 126–141.
- [8] Falk, F., Model Free Energy, Mechanics, and Thermodynamics of SMA, *Acta Metallurgica*, **28**, 1980, 1773–1780.
- [9] Falk, F. & Konopka, P., Three-Dimensional Landau Theory Describing the Martensitic Phase Transformation of SMA, *J. Phys.: Condens. Matter*, **2**, 1990, 61–77.
- [10] Fremond, M., Shape Memory Alloys. A Thermomechanical Model, in *Free Boundary Problems: Theory and Applications*, Eds.: K.-H. Hoffmann & J. Sprekels, Longman Scientific & Technical, 1990, 295–306.
- [11] Glass, D.E. and Tamma, K.K., Non-Fourier Dynamic Thermoelasticity with Temperature-Dependent Thermal Properties, *Journal of Thermophysics and Heat Transfer*, **8**, No. 1, 1994, 145–151.
- [12] Hoffmann, K.-H., Niezgodka, M. & Songmu, Z., Existence and Uniqueness of Global Solutions to an Extended Model of the Dynamic Developments in SMA, *Nonlinear Analysis: TMA*, **15**, No. 10, 1990, 977–990.
- [13] Hoffmann, K.-H. and Zou, J., Finite Element Approximations of Landau-Ginzburg's Equation Model for Structural Phase Transitions in Shape Memory Alloys, *M²AN*, **29**, No. 6, 1995, 629–655.
- [14] Huo, Y., Muller, I. and Seelecke, S. Quasiplasticity and Pseudoelasticity in Shape Memory Alloys, in *Phase Transition and Hysteresis*, ed. by Brokate et al, Springer-Verlag, 1994, 87–146.
- [15] Klein, O., Stability and Uniqueness Results for a Numerical Approximation of the Thermomechanical Phase Transitions in SMA, *Advances in Mathematical Sciences and Applications (Tokyo)*, **5**, No. 1, 1995, 91–116.
- [16] Melnik, R.V.N., Steklov's Operator Technique in Coupled Dynamic Thermoelasticity, *Numerical Methods in Thermal Problems*, Vol. X, Eds. R.W. Lewis & J.T. Cross, 1997, 139–150.
- [17] Moynes, S., Boubakar, M.L. & C. LExcellent, Extension of a Linear Behaviour Model of SMA for Finite Strain Studies, *J. Phys. IV France, Colloque C5*, **7**, 1997, 83–88.
- [18] Muller, I. & T. Ruggeri, *Extended Thermodynamics*, Springer-Verlag, 1993.
- [19] Niezgodka, M. & Sprekels, J., Existence of Solutions for a Mathematical Model of Structural Phase Transitions in SMA, *Math. Methods in the Applied Sciences*, **10**, 1988, 197–223.
- [20] Niezgodka, M. & Sprekels, J., Convergent Numerical Approximations of the Thermomechanical Phase Transitions in SMA, *Numer. Math.*, **58**, 1991, 759–778.
- [21] Nittono, O & Y. Koyama, Japan. J. Appl. Phys., **21**, 1982, 680.
- [22] Renardy, M., Hrusa, W. J. and Nohel, J. A., *Mathematical Problems in Viscoelasticity*, Longman Scientific & Technical, 1987.
- [23] Racke, R. and Zheng, S., Global Existence and Asymptotic Behaviour in Nonlinear Thermoviscoelasticity, *Journal of Differential Equations*, **134**, 1997, 46–67.
- [24] Roberts, A.J., The invariant manifold of beam deformations. Part 1: the simple circular rod, *J. Elas.*, **30**, 1993, 1–54.
- [25] Roberts, A.J., Boundary Conditions for Approximate Differential Equations, *J. Austral. Math. Soc. Ser. B.*, **34**, 1992, 54–80.

- [26] Sijbrand, J., Properties of center manifolds, *Trans. Amer. Math. Soc.*, **289**, 1985, 431-469.
- [27] Sprekels, J., Global Existence for Thermomechanical Processes with Nonconvex Free Energies of Ginzburg-Landau Form, *J. of Math. Analysis and Appl.*, **141**, 1989, 333-348.
- [28] Sprekels, J., Shape Memory Alloys: Mathematical Models for a Class of First Order Solid-Solid Phase Transitions in Metals, *Control and Cybernetics*, **19**, No. 3-4, 1990, 287-308.